Mon. Not. R. Astron. Soc. **276,** 592–596 (1995)

Anisotropic emission, stellar population and X-ray sources in the Seyfert 2 galaxy ESO 138 – G01

Henrique R. Schmitt★ †‡§ and Thaisa Storchi-Bergmann¶
Departamento de Astronomia, IF-UFRGS, CP 15051, CEP 91501-970, Porto Alegre, RS, Brasil

Accepted 1995 April 20. Received 1995 February 24; in original form 1994 June 10

ABSTRACT

We present narrow-band CCD images of the high-excitation Seyfert 2 galaxy ESO138 – G01, centred on the emission lines [O III] λ5007, Hα + [N II] λλ6548, 6584 and adjacent continua. The continuum-subtracted [O III] image presents an elongated jet-like structure to the west of the nucleus which is only weakly visible in the Hα image, and which we conclude is ionized by the nuclear source. The ionization map shows high excitation at the nucleus and at the 'jet'. The continuum ratio map shows that this galaxy is very blue for its morphological type, consistent with the large contribution of a young stellar population up to 3 kpc from the nucleus. We also propose that ESO138 – G01 is the hard X-ray source previously identified with the nearby galaxy NGC 6621.

Key words: galaxies: individual: ESO138 – G01 – galaxies: jets – galaxies: Seyfert – galaxies: stellar content – X-rays: galaxies.

1 INTRODUCTION

ESO138 – G01 is a low-latitude ($b = -9.44°$) early-type galaxy, classified as E/S0 by Prugniel et al. (1993), who derived a position angle for the major axis of ≈ 160° and total apparent blue magnitude of $B_T = 13.18$. At a distance of 36.5 Mpc ($H_0 = 75$ km s^{-1}), derived from its radial velocity of 2740 km s^{-1} (Fairall 1988), the absolute magnitude is $M_B = -19.63$, and the angular scale is 177 pc arcsec^{-1}. What makes this galaxy particular is its nuclear spectrum, studied by Alloin et al. (1992), who found high ionization ([Fe VII] λλ5721, 6087, [Fe XIV] λ5303 and [Ne V] λ3426), as well as low ionization emission lines ([N I] λ5200 and [O I] λ6300). The emission line ratios fall in the loci of active galaxies in diagnostic diagrams (Baldwin, Phillips & Terlevich 1981; Veilleux & Osterbrock 1987), which implies that these galaxies comprise a high excitation nucleus inside a low luminosity E/S0 galaxy, which is not frequently observed.,

In this work we present narrow-band images centred on the redshifted lines [O III] λ5007 and Hα + [N II] λλ6548, 6584, as well as on adjacent continua, which show that the high excitation emission is not restricted to the nucleus, but is extended towards the west reaching 2.12 kpc from the nucleus. Such extended morphologies for the high excitation gas has been found in a number of Seyfert 2 galaxies and have been considered to be evidence for the anisotropic escape of ionizing radiation from the nucleus (Bower et al. 1994; Wilson et al. 1993; Tadhunter & Tsvetanov 1989; Storchi-Bergmann & Bonatto 1991; Storchi-Bergmann, Wilson & Baldwin 1992; Pogge 1988a,b, 1989; Schmitt, Storchi-Bergmann & Baldwin 1994a). We use the images in the continuum to construct ratio maps which are used to derive information on the stellar population and obscuration. We also discuss the origin of the X-ray emission which has been previously attributed to the nearby galaxy NGC 6221 (Marshall et al. 1979; Wood et al. 1984).

2 OBSERVATIONS

Direct CCD images of ESO138 – G01 were obtained through narrow-band filters centred on the redshifted lines [O III] λ5007, Hα + [N II] λλ6548, 6584 and adjacent continua, on the nights 1993 March 16/17 and 17/18 with the 1.5-m telescope of the Cerro Tololo Interamerican Observatory. A log of the observations is shown in Table 1. We have also observed standard calibration stars from the list of Stone & Baldwin (1983).

★ E-mail: schmitt@stsci.edu
†CNPq fellow.
‡Visiting Astronomer at the Cerro Tololo Interamerican Observatory, operated by the Association of Universities for Research in Astronomy Incorporated, under contract to the National Science Foundation.
§Present address: Space Telescope Science Institute, 3700 San Martin Drive, Baltimore, MD21218, USA.
¶E-mail: thaisa@ifl.if.ufrgs.br

Table 1. CCD images of ESO138 – G01.

Filter (Å/ΔÅ)	Expos. (sec)	Night	Comments	Seeing
5400/100	2700	16/17	continuum	1.3″
5057/15	3600	16/17	[OIII]λ5007	1.3″
6477/72	1200	17/18	continuum	1.4″
6606/76	1400	17/18	Hα+[NII]λλ6548,6584	1.4″

The individual images were corrected for bias, flat-field, and were flux calibrated using standard IRAF procedures. The images were also corrected for atmospheric and galactic extinction $E(B-V)=0.22$, interpolated from the values of Burstein & Heiles (1984). The point-spread function (PSF) of the line plus continuum and the continuum images were compared, and the one with the smaller PSF was convolved with a Gaussian function in order to match the one with the larger PSF. Each continuum image was then scaled by a factor such that the integrated number of counts for the stars in the field was equal to the corresponding value in the line plus continuum frame. Finally, continuum-free images in [O III] and Hα, with resolution of 1.4 arcsec, were produced by subtracting the appropriate continuum frame from the line plus continuum one.

We have also constructed ionization and continuum ratio maps. The ionization maps were constructed dividing the continuum-subtracted [O III] image by the Hα one, in order to study the morphology of the high excitation gas (Pogge 1988a). To eliminate the effect of spurious points, which occur as a result of the division of the [O III] image by values near zero in the external region of the Hα image, the pixels with values lower than 2σ (where σ is the standard deviation of the noise after the sky subtraction) were clipped to a constant value. We have also divided the red by the green continuum image in order to study colour gradients which can give information about the stellar population and/or obscuration (Schmitt et al. 1994a). As we are interested in the nuclear and near nuclear region, we have clipped the green continuum image to 5σ.

3 RESULTS

In Fig. 1 we show contour maps of the final images. In the top panel we show the green (left) and red continuum maps (right). In the middle the continuum-subtracted [O III] (left) and Hα (right) images, and in the bottom panel the ionization (left) and continuum ratio maps (right). The lowest isophotal level corresponds to 2σ above the noise level, and the following ones are 3σ, 5σ, 7σ and 9σ, while above 9σ the contours correspond to values that vary from image to image.

We do not see any evident distortions in the contours of the continuum images which would indicate the presence of spiral arms, confirming the classification as E/S0 by Prugniel et al. (1993). The isophotes have an approximately elliptical shape with orientation consistent with the major axis PA≈160° obtained by Prugniel et al. (1993). No structures similar to spiral arms are seen in the continuum-subtracted Hα image either. It is also possible to observe a large number of foreground stars in the continuum images, due to their low galactic latitude.

The [O III] image has a strikingly different morphology from that of the continuum images: the isophotes present a large extension along the PA 265° (≈west) which could be either due to a jet of material, or gas being illuminated by collimated nuclear light in this direction. This structure reaches a distance of 12 arcsec (2.12 kpc) from the nucleus at the 2σ level, with a peak of emission at 7.3 arcsec (1.3 kpc) from the nucleus. In the opposite direction (east) there is a small extension at the two lowest isophotal levels, which could be due to a counterpart structure (e.g. a 'counter jet') partially hidden by the plane of the galaxy (e.g. NGC 3281 in Storchi-Bergmann, Wilson & Baldwin 1992; NGC 1365 and 7582 in Storchi-Bergmann & Bonatto 1991). Some internal isophotes present a distortion along PA 120°. The total extension of the emission along the direction east–west is 20 arcsec (3.54 kpc) and along the direction north–south is 12 arcsec (2.12 kpc).

The presence of this extended emission in [O III] and also in Hα (although weaker) was confirmed by Bica (1994, private communication) in a long-slit spectrum of this galaxy, obtained at PA 90°.

In the Hα image, the extended emission to the west can only be observed at the 1σ level. It extends by 13 arcsec (2.3 kpc) along the east–west direction and by 8.8 arcsec (1.56 kpc) along the north–south direction. It can also be seen that the internal isophotes are somewhat extended along PA 55°. The fluxes of the emission lines [O III] λ5007 and Hα+[N II] λλ6548, 6584 were integrated over their images using circular apertures of different radius and also integrating all the emission above the 2σ level (total emission). The results are given in Table 2.

In the ionization map we observe the same structure seen in the [O III] image. The regions where it was possible to detect Hα above the 2σ level are plotted with heavier contours, while the other regions have lighter contours. The peak of the ionization map is displaced by 1.5 arcsec towards the south of the nucleus. The extended structure to the west also has high excitation, with a peak at 7.3 arcsec west. Although the value in the ionization map at this region is ≈50 per cent of that of the nucleus, we point out that Hα was not detected at 2σ in this structure, suggesting an even higher excitation.

In the lower right panel of Fig. 1 we show the continuum ratio map. Such a map is sensitive both to stellar population gradients and reddening. In order to separate the two effects, we have used stellar population templates from the library of Bica (1988) to derive the continuum ratio λ6477 Å/λ5400 Å, using the transmission curves of the filters used to observe the galaxy. In Table 3 we show the calculated ratio λ6477 Å/λ5400 Å for the templates S1 and S7. These templates correspond to increasing contribution of young components, from S1 (0 per cent) to S7 (70 per cent). The templates S1 to S4 have approximately the same value for the continuum ratio, while for S5, S6 and S7 this value gradually decreases. The values of the continuum ratios of ESO138 – G01 decrease towards the nucleus (dashed lines), where its value is 1.0, which is typical of a young stellar population S7. From the nucleus up to a radius of 2.5 arcsec

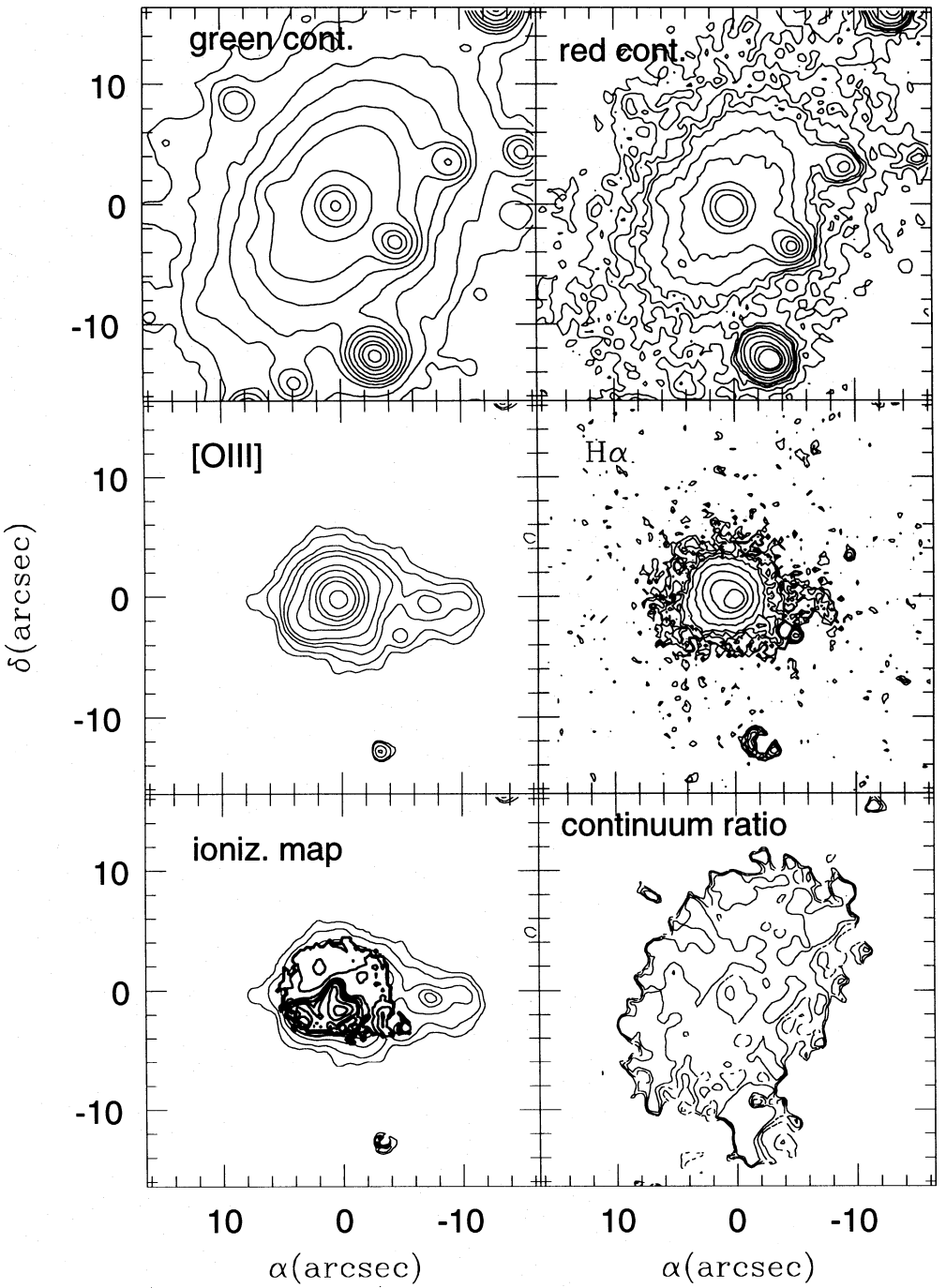

Figure 1. Isophotal contours of ESO138−G01 images: green continuum (upper left), red continuum (upper right), continuum-subtracted [O III] (middle left), continuum-subtracted Hα (middle right), ionization map (lower left), continuum ratio map (lower right). The lower level corresponds to 2σ. North is to the top and east to the left. The heavier contours in the ionization map indicate locations where the Hα image is observed above the 2σ level. The dashed lines in the continuum ratio map show the lower contour levels (1.0 and 1.1).

this value increases to 1.1, which is an average between the values of the templates S6 and S7. An alternative explanation could be that the nucleus is blue due to the continuum of the active nucleus and the circumnuclear regions are also blue due to scattered nuclear light. Nevertheless, Alloin et al. (1992), from a spectrum obtained within an aperture of 1.5×5.8 arcsec^2, derive a stellar population whose characteristics are exactly the same as the ones from an S6/S7 template. Farther out we find some regions where the value of the continuum ratio is 1.2 (solid lines). This value can be due to either an older stellar population ($\approx$ S5 template), or to the same population as the inner part reddened by $E(B-V) \approx 0.3$. In either case, we conclude that this galaxy is very blue, apparently due to the blueness contribution from young stars spread along the inner ≈ 3 kpc of the galaxy, which is a peculiar characteristic for an E/S0 galaxy.

Table 2. Emission-line fluxes.

Aperture Radius	[OIII]λ5007 Flux 10^{-13}ergs cm^{-2} s^{-1}	Hα+[NII]λλ6548,6584 Flux 10^{-13}ergs cm^{-2} s^{-1}
1″	4.13	1.51
2″	7.64	2.97
3″	8.63	3.60
4″	9.08	3.86
5″	9.33	4.0
total	9.72	4.19

Table 3. Continuum ratio of the templates.

Template	λ6477Å/λ5400Å
S1	1.266
S2	1.262
S3	1.236
S4	1.235
S5	1.198
S6	1.161
S7	1.007

4 X-RAY EMISSION

ESO138 – G01 is located at 15 and 11 arcmin from NGC 6215 and 6221, respectively, which have starburst like nuclei (Bonatto, Bica & Alloin 1989; Kinney et al. 1993). Marshall et al. (1979) and Wood et al. (1984) found an X-ray source in the *HEAO A-2* and *HEAO A-1* satellite surveys close to the location of NGC 6221. Pence & Blackman (1984) and Véron, Véron & Zuiderwijk (1981) found, based on high-dispersion spectra, a Seyfert component in the nucleus of NGC 6221. Because of the presence of this component, they suggested that the X-ray source was NGC 6221. Nevertheless, we have noticed that the position of this galaxy is outside the observational error boxes. Comparing the position of these error boxes and the position of NGC 6221, 6215 and ESO138 – G01, it can be seen that ESO138 – G01 is the only one inside them, indicating that the identification of NGC 6221 with the X-ray source is possibly wrong and that it is more likely to correspond to ESO138 – G01. Above all, we have noticed that the Seyfert component in the NGC 6221 spectrum is rather weak, its emission line ratios being more typical of H II regions (Schmitt et al. 1994b), while ESO138 – G01 has a high excitation spectrum (Alloin et al. 1992).

In order to further test the hypothesis that the hard X-ray source is related to ESO138 – G01 instead of NGC 6221, we have compared the ratio log([O III]/hard X-ray) with the mean value of Seyfert 2 galaxies −1.76, with variance 0.38, given by Malchaey et al. (1994). For NGC 6221 we have used the hard X-ray flux 5×10^{-11} erg cm^{-2} s^{-1}, obtained from the luminosity given by Marshall et al. (1979), and the [O III] λ5007 flux of 6.17×10^{-14} erg cm^{-2} s^{-1} (Whittle 1992), which gives the ratio log([O III]/hard X-ray) = −2.91. For ESO138 – G01 we used the same hard X-ray flux and our measured [O III] fluxes from Table 2, which gives the ratio log([O III]/hard X-ray) = −2.08 for the [O III] flux integrated over a circular aperture of 1 arcsec radius and −1.71 for the total [O III] flux. We see that for NGC 6221 this ratio differs from the average value given by Mulchaey et al. (1994) by approximately three times the variance, while for ESO138 – G01 it agrees with the average value within the variance. This result reinforces the identification of ESO138 – G01 with the hard X-ray source.

5 CONCLUSIONS

In this paper we confirm, based on narrow-line images centred on the emission lines [O III] and Hα, that the galaxy ESO138 – G01 has a high excitation nucleus, typical of Seyfert 2 galaxies. We have also detected a high excitation jet-like structure extending up to ≈2 kpc from the nucleus, which presents strong [O III] emission, weak Hα, and is not visible in the continuum images. The above characteristics lead us to conclude that it is either gas ejected from the active nucleus and ionized by it, or gas previously present on that location being ionized by an anisotropic nuclear source. From the continuum ratio map we can conclude that the nucleus is very blue, consistent with a young stellar population as derived from previous spectroscopic observations. But a remarkable result is that the continuum is similarly blue up to 3 kpc from the nucleus, suggesting that the contribution from young stars extends to a large distance.

We also conclude that ESO138 – G01 is probably the hard X-ray source previously identified with the nearby galaxy NGC 6221, as the former galaxy has a much higher ionization spectrum, is closest to the position of the X-ray source and fits better into the relation between hard X-ray and [O III] line fluxes for Seyfert galaxies.

The results of this paper suggest that ESO138 – G01 could be another Seyfert galaxy that fits in the Unified AGN Model proposed by Antonucci & Miller (1985). In order to confirm the conclusions about the X-ray source in this galaxy it would be important to observe it again in X-rays (e.g. with *ROSAT* or *ASCA*). It would also be interesting to observe the 'jet' through high-resolution radio observations, as well as high-resolution, high signal-to-noise long-slit spectra of this galaxy, which could reveal if the active nucleus is hidden from direct view through photon balance calculations (e.g. Schmitt et al. 1994a; Storchi-Bergmann et al. 1992).

ACKNOWLEDGMENTS

We would like to thank E. Bica for valuable information about his long-slit spectrum, C. J. Bonatto for a critical reading of the manuscript and also an anonymous referee for valuable suggestions. This work was partially supported by the Brazilian institutions CNPq, FINEP and FAPERGS.

REFERENCES

Alloin D., Bica E., Bonatto C. J., Prugniel P., 1992, A&A, 266, 117
Antonucci R. R. J., Miller J. S., 1985, ApJ, 297, 621
Baldwin J. A., Phillips M. M., Terlevich R., 1981, PASP, 93, 5
Bica E., 1988, A&A, 195, 76
Bonatto C., Bica E., Alloin D., 1989, A&A, 226, 23
Bower G. A., Wilson A. S., Mulchaey J. S., Miley G. K., Heckmann T. M., Krolik J. H., 1994, AJ, 107, 1686
Burstein D., Heiles C., 1984, ApJS, 54, 33
Fairall A. P., 1988, MNRAS, 230, 69
Kinney A. L., Bohlin R. C., Calzetti D., Panagia N., Wyse R. F. G., 1993, ApJS, 86, 5
Marshall F. E., Boldt E. A., Holt S. S., Mushotzky R. F., Pravdo S. H., Rotschild R. E., Serlemitsos P. J., 1979, ApJS, 40, 657
Mulchaey J. S., Koratkar A., Ward M. J., Wilson A. S., Whittle M., Antonucci R. R. J., Kinney A. L., Hurt T., 1994, ApJ, 436, 586
Pence W. D., Blackman C. P., 1984, MNRAS, 207, 9
Pogge R. W., 1988a, ApJ, 328, 519
Pogge R. W., 1988b, ApJ, 332, 702
Pogge R. W., 1989, ApJ, 345, 730
Prugniel Ph., Bica E., Klotz A., Alloin D., 1993, A&AS, 98, 229
Schmitt H. R., Storchi-Bergmann T., Baldwin J. A., 1994a, ApJ, 423, 237
Schmitt H. R., Storchi-Bergmann T., Wilson A. S., Baldwin J. A., 1994b, in Tenorio-Tagle G., ed., Star Formation in the Universe. Cambridge, p. 325
Stone R. P. S., Baldwin J. A., 1983, MNRAS, 204, 347
Storchi-Bergmann T., Bonatto C. J., 1991, MNRAS, 250, 138
Storchi-Bergmann T., Wilson A. S., Baldwin J. A., 1992, ApJ, 396, 45
Tadhunter C. N., Tsvetanov Z., 1989, Nat, 341, 422
Veilleux S., Osterbrock D. E., 1987, ApJS, 63, 295
Véron M. P., Véron P., Zuiderwijk E. J., 1981, A&A, 98, 34
Whittle M., 1992, ApJS, 79, 49
Wilson A. S., Braatz J. A., Heckman T. M., Krolik J. H., Miley G. K., 1993, ApJ, L61
Wood K. S., Meekins J. F., Yentis D. J., Smathers H. W., McNutt D. P., Bleach R. D., Byran E. T., Friedman H., Meidav M., 1984, ApJS, 56, 507